

Vector wave diffraction pattern of slits masked by polarizing devices

MOHAMMAD TAHIR^{1,*}, K BHATTACHARYA² and
A K CHAKRABORTY²

¹Jhikra High School (H.S.), Jhikra, Joypur, Howrah 711 401, India

²Department of Applied Optics and Photonics, Calcutta University, 92 Acharya Prafulla Chandra Road, Kolkata 700 009, India

*Corresponding author. E-mail: mail2mdtahir@gmail.com

MS received 11 July 2011; revised 4 October 2011; accepted 21 October 2011

Abstract. Polarization property is important to the optical imaging system. It has recently been understood that the polarization properties of light can be fruitfully used for improving the characteristics of imaging system that includes polarizing devices. The vector wave imagery lends an additional degree of freedom that can be utilized for obtaining results that are unobtainable in scalar wave imagery. This calls for a systematic study of diffraction properties of different apertures using polarization-sensitive devices. In the present paper, we have studied the Fraunhofer diffraction pattern of slits masked by different kinds of polarizing devices which introduce a phase difference between the two orthogonal components of the incident beam.

Keywords. Polarization Fourier optics; diffraction of polarized light.

PACS Nos 42.25.Ja; 42.25.Fx

1. Introduction

The interference pattern produced by the superposition of waves depends not only on the degree of coherence between the interfering beams but also on their states of polarization. We know that the phenomenon of diffraction is essentially the effects of interference of secondary wavelets originating from all points of the wave confined by the diffracting aperture. It is, therefore, well expected that the variation of polarization of the wave on the diffracting aperture will alter both the near-field and far-field diffraction patterns.

Before recognizing the fact that polarization properties of light waves can play a vital role in optical imagery, scalar wave properties of light were usually considered to tailor the characteristics of optical imaging systems. Amplitude and phase step filters were used on the pupil of the optical system to achieve the required modifications. But in conventional imaging system, the diffraction properties change only marginally if the state of

polarization of the input beam changes. This justifies the use of scalar diffraction theory to study the optical imaging system.

But recent studies on the use of polarization masks in imaging systems, however, call for a more general theory of diffraction that takes polarization effects into account which have been studied by several authors [1–7]. It is shown that the utilization of polarization devices in an imaging system considerably improves the performance characteristics of the system and provides additional degrees of freedom that enable one to effectively modify the imaging characteristics in a pre-specified manner. Studies of vector wave imagery have revealed that the use of polarization properties of light increases the versatility of the imaging system and have many useful applications which cannot be addressed by scalar theory of light. Besides, the imaging properties of such a system can be varied continuously by varying the orientation of any polarizing devices included in the system or by changing the state of polarization of the incident beam.

In the field of image and image processing, Fourier analysis is being so extensively used that a new branch of optics, known as ‘Fourier Optics’ has emerged. In Fourier optics, we usually ignore the vector nature of light. Most of the studies relating to Fourier optics made so far are based on the scalar nature of light. It is well known that the Fraunhofer diffraction pattern of an object transparency is given by the Fourier transform of the transmission function of the object. The Fourier transform of the far-field diffraction pattern gives the image of the object. Thus both the far-field diffraction pattern and the theory of imagery come under the purview of what is known as Fourier optics. The branch of Fourier optics devoted to the study of vector wave diffraction and imagery is known as ‘Polarization Fourier Optics’. A substantial amount of work has been done in the field of polarization Fourier optics dealing with vector wave imagery and image processing [8–10].

Recently, Moreno *et al* have extended the scalar Fourier optics to the vector theory by using Jones matrix formalism and analysed the variable intensity and polarization distribution in the Fourier plane for a typical aperture having polarizing devices used as masks. As a matter of fact, they have studied the variation of the state of polarization in the far-field pattern of a slit masked by two orthogonal polarizers [11]. In the present paper we have studied in the first case the far-field diffraction pattern of a slit placed in tandem with a birefringent wedge that introduces a linear phase variation between the two orthogonal components of the beam incident on the slit. In the second case, we have studied the effect of two identical slits separated by a distance (one of the slit is masked by a retarder).

2. Theory

Case 1. Let a birefringent wedge be placed in front of the slit aperture of width d as shown in figure 1. The edge of the birefringent wedge is assumed to be parallel to the length of the slit. The phase difference introduced by the birefringent wedge is given by

$$\phi(x) = 2\pi/\lambda (n_e - n_o)t(x), \quad (1)$$

where $t(x)$ is the wedge thickness at x .

It may be mentioned that the nature of diffraction pattern produced by the combination of the birefringent wedge and the slit does not depend on the absolute values of the phase but depends on the phase difference introduced by the wedge which varies across the slit.

Vector wave diffraction pattern of slits

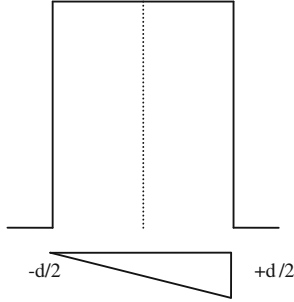


Figure 1. A single slit and a birefringent wedge.

If the phase difference introduced by the wedge between the two orthogonal components is $n\pi$ at the centre of the slit and $2n\pi$ at the two ends of the slit, we can write the phase difference in the form

$$\phi(x) = 2n\pi \frac{x}{d} + n\pi \quad (2)$$

so that $\phi(x)$ varies from 0 to $2n\pi$ across the slit.

That is, the birefringent wedge introduces phase difference at different values of x such that

$$\begin{aligned} \phi(0) &= n\pi, & \text{at } x &= 0, \\ \phi\left(-\frac{d}{2}\right) &= \phi(0) - n\pi, & \text{at } x &= -\frac{d}{2}, \end{aligned}$$

and

$$\phi\left(\frac{d}{2}\right) = \phi(0) + n\pi, \quad \text{at } x = \frac{d}{2}.$$

Thus the transmission function of the birefringent wedge may be expressed in terms of the given Jones matrix.

$$L = \begin{vmatrix} 1 & 0 \\ 0 & \exp i(\phi(x)) \end{vmatrix}, \quad (3)$$

where $\phi(x)$ is given by eq. (2). Conventionally x -axis is considered as the fast axis and y -axis as the slow axis of the wedge.

In order to study the diffraction properties of the slit masked by the birefringent wedge, we assume that the input beam or the beam coming from the object is elliptically polarized in general. It may be represented by the Jones vector

$$\varepsilon_i = \begin{vmatrix} a \\ b \exp(i\delta_0) \end{vmatrix}. \quad (4)$$

Now the slit used may be represented by the rectangular function,

$$\begin{aligned} \text{rect}\left(\frac{x}{d}\right) &= 1 & \text{for } -d/2 \leq x \leq d/2 \\ &= 0 & \text{elsewhere.} \end{aligned} \quad (5)$$

Thus, the vector wave amplitude just behind the slit may be written as

$$\begin{aligned}\varepsilon_0 &= \text{rect}\left(\frac{x}{d}\right) \varepsilon_i L \\ &= \text{rect}\left(\frac{x}{d}\right) \left| \begin{array}{cc} 1 & 0 \\ 0 & \exp(i(\phi(x))) \end{array} \right| \left| \begin{array}{c} a \\ b \exp(i\delta_0) \end{array} \right| \\ &= \text{rect}\left(\frac{x}{d}\right) \left| \begin{array}{c} a \\ b \exp(i(\delta_0 + \phi(x))) \end{array} \right|.\end{aligned}\quad (6)$$

The vector wave amplitude distribution $F(u)$ in the Fraunhofer diffraction pattern is obtained by taking the Fourier transform of eq. (6).

$$F(u) = \left| \begin{array}{c} \frac{ad \sin \pi ud}{\pi ud} \\ (-1)^n b \exp(i\delta_0) d \frac{\sin(\pi ud + n\pi)}{(\pi ud + n\pi)} \end{array} \right|.$$

In the absence of the analyser at the output side the intensity distribution may be written as

$$I(X)_{\text{NA}} = d^2 \left[\frac{a^2 \sin^2 X}{X^2} + \frac{b^2 \sin^2(X + n\pi)}{(X + n\pi)} \right], \quad (7)$$

where $X = \pi ud$ is the observation plane coordinate.

If an analyser $P(\theta)$ is placed at the output side whose transmission axis makes an angle θ with the chosen x -axis, the vector wave amplitude obtained at the observation plane is then given by

$$F(u)_{\text{WA}} = P(\theta)F(u),$$

where

$$P(\theta) = \left| \begin{array}{cc} \cos^2 \theta & \sin \theta \cos \theta \\ \sin \theta \cos \theta & \sin^2 \theta \end{array} \right|.$$

Therefore, the vector amplitude distribution at the observation plane is given by

$$F(u)_{\text{WA}} = d^2 \left| a \frac{\sin X}{X} \cos \theta + (-1)^n b \exp(i\delta_0) \frac{\sin(X + n\pi)}{(X + n\pi)} \sin \theta \right| \left| \begin{array}{c} \cos \theta \\ \sin \theta \end{array} \right|.$$

The intensity distribution may be written as

$$\begin{aligned}I(X)_{\text{WA}} &= d^2 \left| a \frac{\sin X}{X} \cos \theta + (-1)^n b \exp(i\delta_0) \frac{\sin(X + n\pi)}{(X + n\pi)} \sin \theta \right|^2 \\ &= d^2 \left[a^2 \frac{\sin^2 X}{X^2} \cos^2 \theta + b^2 \frac{\sin^2(X + n\pi)}{(X + n\pi)^2} \sin^2 \theta \right. \\ &\quad \left. + ab(-1)^n \frac{\sin X}{X} \frac{\sin(X + n\pi)}{(X + n\pi)} \sin 2\theta \cos \delta_0 \right].\end{aligned}\quad (8)$$

2.1 Computation and discussion

The theoretical analysis presented above shows that the Fraunhofer diffraction pattern of a slit gets considerably modified if a birefringent wedge masks the slit. We have calculated the intensity distribution obtained in the Fourier plane and presented it in a graphical

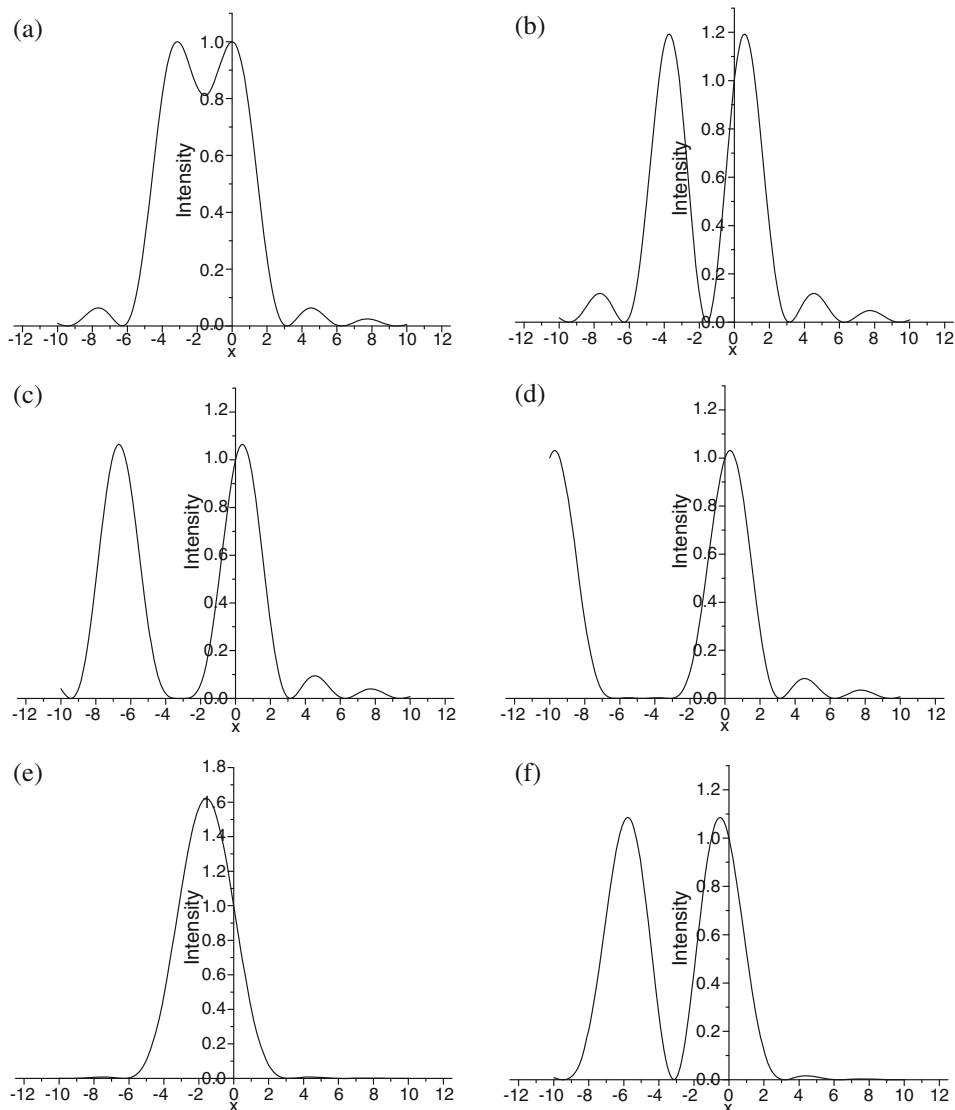


Figure 2. Variation of intensity with X (a) without analyser at the output and when $a = 1, b = 1, n = 1$, (b) when $a = 1, b = 1, \delta_0 = 0^\circ, n = 1, \theta = 45^\circ$, (c) when $a = 1, b = 1, \delta_0 = 0^\circ, n = 2, \theta = 45^\circ$, (d) when $a = 1, b = 1, \delta_0 = 0^\circ, n = 3, \theta = 45^\circ$, (e) when $a = 1, b = 1, \delta_0 = 0^\circ, n = 1, \theta = -45^\circ$, (f) when $a = 1, b = 1, \delta_0 = 0^\circ, n = 2, \theta = -45^\circ$, (g) when $a = 1, b = 1, \delta_0 = 0^\circ, n = 3, \theta = -45^\circ$, (h) when $a = 1, b = 1, \delta_0 = 0^\circ, n = 1, \theta = 30^\circ$ and (i) when $a = 1, b = 1, \delta_0 = 90^\circ, n = 1, \theta = 30^\circ$.

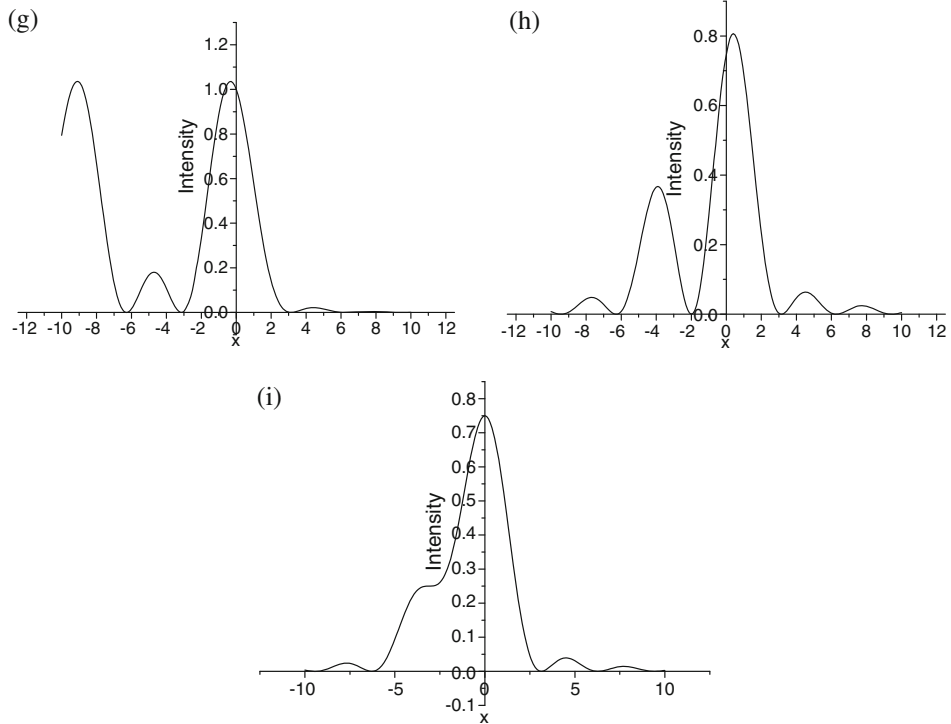


Figure 2. Continued.

form. It is clear that the intensity pattern depends on the state of polarization of the incident beam, the phase difference introduced by the wedge and the analyser angle θ . When no analyser is placed at the output side, the distribution pattern obtained is as depicted in figure 2a. It shows two peaks with a hump in between. In the absence of the analyser, both the orthogonal components of the beam will produce their own distribution patterns and the resultant Fraunhofer diffraction pattern will be an incoherent superposition of the diffraction patterns produced by two individual components of the beam used. Since there is a linear variation of phase difference introduced between the two orthogonal components, the Fraunhofer diffraction due to one component will be shifted with respect to that due to the other component. When an analyser is used at the output side, the analyser selects a component of each of the orthogonal components of the beam. The two components selected by the analyser will then interfere and the redistribution of intensity will occur at the Fraunhofer diffraction pattern. Figures 2b–2i depict the nature of variation obtained for different values of δ_0 , n and the analyser angle θ . It is interesting to note that when the analyser angle is -45° with the x -axis and $a = 1$, $b = 1$, $\delta_0 = 0^\circ$, $n = 1$, the secondary lobes in the diffraction pattern have been suppressed almost completely as seen in figure 2e. This is analogous to apodization obtained in circular aperture using Gaussian modulation of the transmission function of a circular aperture.

Case 2. Let two identical parallel apertures, each of width d , be separated by a distance $2r$ as shown in figure 3. Let an elliptically polarized beam be incident on these apertures.

The Jones matrix of the incident beam is

$$\varepsilon_i = \begin{vmatrix} a \\ b \exp(i\delta_0) \end{vmatrix}, \quad (9)$$

where a, b are the amplitudes of the x and y components of the incident beam and δ_0 is the initial phase difference between them. Let the first aperture be unmasked and the second aperture be masked by the retarder whose fast axis is considered as the x -axis and slow axis as the y -axis.

The Jones matrix of the retarder is

$$C(\delta) = \begin{vmatrix} 1 & 0 \\ 0 & \exp(i\delta) \end{vmatrix}, \quad (10)$$

where δ is the phase introduced by the retarder between the x and y components of the incident beam.

The vector wave-field just behind the two identical parallel apertures is

$$\begin{aligned} \varepsilon_0 &= \text{rect}\left(\frac{x-r}{d}\right) \begin{vmatrix} a \\ b \exp(i\delta_0) \end{vmatrix} \\ &\quad + \text{rect}\left(\frac{x+r}{d}\right) \exp(i\Delta_0) \begin{vmatrix} 1 & 0 \\ 0 & \exp(i\delta) \end{vmatrix} \begin{vmatrix} a \\ b \exp(i\delta_0) \end{vmatrix} \\ &= \text{rect}\left(\frac{x-r}{d}\right) \begin{vmatrix} a \\ b \exp(i\delta_0) \end{vmatrix} \\ &\quad + \text{rect}\left(\frac{x-r}{d}\right) \exp(i\Delta_0) \begin{vmatrix} a \\ b \exp(i(\delta + \delta_0)) \end{vmatrix}. \end{aligned} \quad (11)$$

Now the aperture may be represented by the rectangular function

$$\begin{aligned} \text{rect}\left(\frac{x}{d}\right) &= 1, \quad \text{for } -\frac{d}{2} \leq x \leq \frac{d}{2} \\ &= 0, \quad \text{elsewhere.} \end{aligned}$$

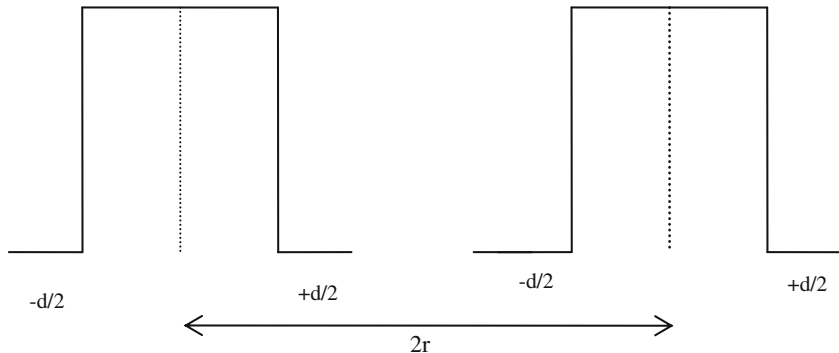


Figure 3. Double slit separated by a distance $2r$.

The vector wave amplitude distribution in the Fraunhofer distribution pattern $F(u)$ is obtained by taking the Fourier transform of eq. (11). So

$$F(u) = \frac{\sin \pi u d}{\pi u d} \exp(i 2 \pi u r) \left| \begin{array}{c} a \\ b \exp(i \delta_0) \end{array} \right| + \frac{\sin \pi u d}{\pi u d} \exp(-i 2 \pi u r) \exp(i \Delta_0) \left| \begin{array}{c} a \\ b \exp(i(\delta + \delta_0)) \end{array} \right|.$$

This diffraction pattern is characterized by the Jones matrix such as

$$\begin{aligned} F(u) &= \frac{\sin \pi u d}{\pi u d} \left| \begin{array}{c} a[\exp(i 2 \pi u r) + \exp(-i 2 \pi u r) \exp(i \Delta_0)] \\ b \exp(i \delta_0)[\exp(i 2 \pi u r) + \exp(-i 2 \pi u r) \exp(i(\delta_0 + \delta + \Delta_0))] \end{array} \right| \\ &= 2 \frac{\sin \pi u d}{\pi u d} \left| \begin{array}{c} a \exp i \left(\frac{\Delta_0}{2} \right) \cos \left(2 \pi u r - \frac{\Delta_0}{2} \right) \\ b \exp \left[i \left\{ \delta_0 + \frac{(\delta_0 + \delta + \Delta_0)}{2} \right\} \right] \cos \left[2 \pi u r - \frac{(\delta_0 + \delta + \Delta_0)}{2} \right] \end{array} \right|. \end{aligned} \quad (12)$$

When an analyser is placed at the output side, the intensity distribution pattern obtained is given by

$$\begin{aligned} I(u) &= |F(u)|^2 = 4 \frac{\sin^2(\pi u d)}{(\pi u d)^2} \\ &\times \left[a^2 \cos^2 \left(2 \pi u r - \frac{\Delta_0}{2} \right) + b^2 \cos^2 \left\{ 2 \pi u r - \frac{(\delta_0 + \delta + \Delta_0)}{2} \right\} \right]. \end{aligned}$$

Assuming $X = \pi u d$ the intensity distribution pattern is

$$\begin{aligned} I(u) &= I(X) = 4 \frac{\sin^2 X}{X^2} \\ &\times \left[a^2 \cos^2 \left(4X - \frac{\Delta_0}{2} \right) + b^2 \cos^2 \left\{ 4X - \frac{(\delta_0 + \delta + \Delta_0)}{2} \right\} \right]. \end{aligned} \quad (13)$$

If an analyser is placed at the output side whose transmission axis makes an angle θ with the x -axis, the intensity distribution may be written as

$$\begin{aligned} I(u, \theta) &= 4 \frac{\sin^2(\pi u d)}{(\pi u d)^2} \left| \left[a \exp \left(i \frac{\Delta_0}{2} \right) \cos \left(2 \pi u r - \frac{\Delta_0}{2} \right) \right] \cos \theta \right. \\ &\quad \left. + \left[b \exp \left\{ i \left(\delta_0 + \frac{(\delta_0 + \delta + \Delta_0)}{2} \right) \right\} \right] \right. \\ &\quad \left. \times \cos \left\{ 2 \pi u r - \frac{(\delta_0 + \delta + \Delta_0)}{2} \right\} \right] \sin \theta \right|^2 \end{aligned}$$

or

$$I(u, \theta) = 4 \frac{\sin^2(\pi u d)}{(\pi u d)^2} \left[a^2 \cos^2 \left(2\pi u r - \frac{\Delta_0}{2} \right) \cos^2 \theta \right. \\ \left. + b^2 \cos^2 \left\{ 2\pi u r - \frac{(\delta_0 + \delta + \Delta_0)}{2} \right\} \sin^2 \theta \right. \\ \left. + ab \cos \left(2\pi u r - \frac{\Delta_0}{2} \right) \cos \left\{ 2\pi u r - \frac{(\delta_0 + \delta + \Delta_0)}{2} \right\} \right. \\ \left. \times \cos \left(\frac{3\delta_0}{2} + \frac{\delta}{2} + \Delta_0 \right) \sin 2\theta \right].$$

Assuming $r = 2d$ and $\pi u d = X$, the intensity distribution in the Fourier plane is

$$I(X, \theta) = 4 \frac{\sin^2 X}{X^2} \left[\begin{array}{l} a^2 \cos^2 \left(4X - \frac{\Delta_0}{2} \right) \cos^2 \theta \\ + b^2 \cos^2 \left\{ 4X - \frac{(\delta_0 + \delta + \Delta_0)}{2} \right\} \sin^2 \theta \\ + ab \cos \left(4X - \frac{\Delta_0}{2} \right) \\ \times \cos \left\{ 4X - \frac{(\delta_0 + \delta + \Delta_0)}{2} \right\} \\ \times \cos \left(\frac{3\delta_0}{2} + \frac{\delta}{2} + \Delta_0 \right) \sin 2\theta \end{array} \right]. \quad (14)$$

If we assume $2r = d$, the two apertures come in contact with one another. Therefore, it is a particular case of the previous example, where the width of the rectangles is equal to their separation. In this case the intensity distribution is given by

$$I(X, \theta) = 4 \frac{\sin^2 X}{X^2} \left[\begin{array}{l} a^2 \cos^2 \left(X - \frac{\Delta_0}{2} \right) \cos^2 \theta \\ + b^2 \cos^2 \left\{ X - \frac{(\delta_0 + \delta + \Delta_0)}{2} \right\} \sin^2 \theta \\ + ab \cos \left(X - \frac{\Delta_0}{2} \right) \\ \times \cos \left\{ X - \frac{(\delta_0 + \delta + \Delta_0)}{2} \right\} \\ \times \cos \left(\frac{3\delta_0}{2} + \frac{\delta}{2} + \Delta_0 \right) \sin 2\theta \end{array} \right]. \quad (15)$$

2.2 Computation and discussion

The theoretical analysis presented here shows that the Fraunhofer diffraction pattern of two identical parallel apertures gets also considerably modified by the polarization properties of light. We have calculated the intensity distribution obtained and presented it in a graphical form. From eq. (14), it is clear that the intensity pattern depends on the parameters a , b , δ_0 and the analyser angle θ . When no analyser is placed at the output side, the

distribution pattern obtained is as depicted in figure 4a. This curve is equivalent to that produced by the single aperture of width d . When the analyser is oriented at $\theta = 0^\circ$ the diffraction pattern is independent of the state of polarization and the retardance (δ). In

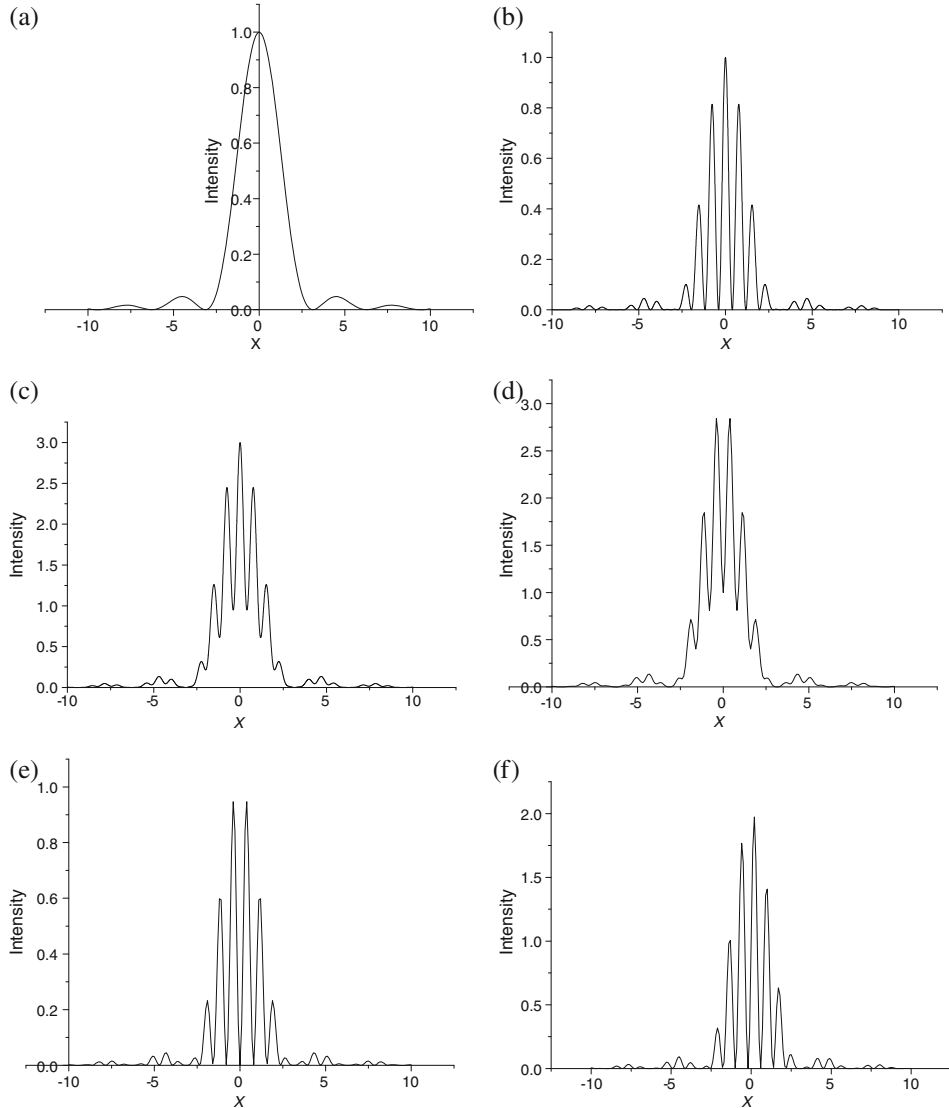


Figure 4. Variation of intensity with X (a) without analyser at the output, (b) when $\theta = 0^\circ$, $\Delta_0 = 0$, (c) when $a = 1$, $b = 1$, $\delta_0 = 0^\circ$, $\delta = 180^\circ$, $\Delta_0 = 0$, $\theta = 30^\circ$, (d) when $a = 1$, $b = 1$, $\delta_0 = 0^\circ$, $\delta = 180^\circ$, $\Delta_0 = 0$, $\theta = 60^\circ$, (e) when $a = 1$, $b = 1$, $\delta_0 = 0^\circ$, $\delta = 180^\circ$, $\Delta_0 = 0$, $\theta = 90^\circ$ or $a = 1$, $b = 1$, $\delta_0 = 90^\circ$, $\delta = 90^\circ$, $\Delta_0 = 0$, $\theta = 90^\circ$ and (f) when $a = 1$, $b = 1$, $\delta_0 = 90^\circ$, $\delta = 180^\circ$, $\Delta_0 = 0$, $\theta = 90^\circ$.

Vector wave diffraction pattern of slits

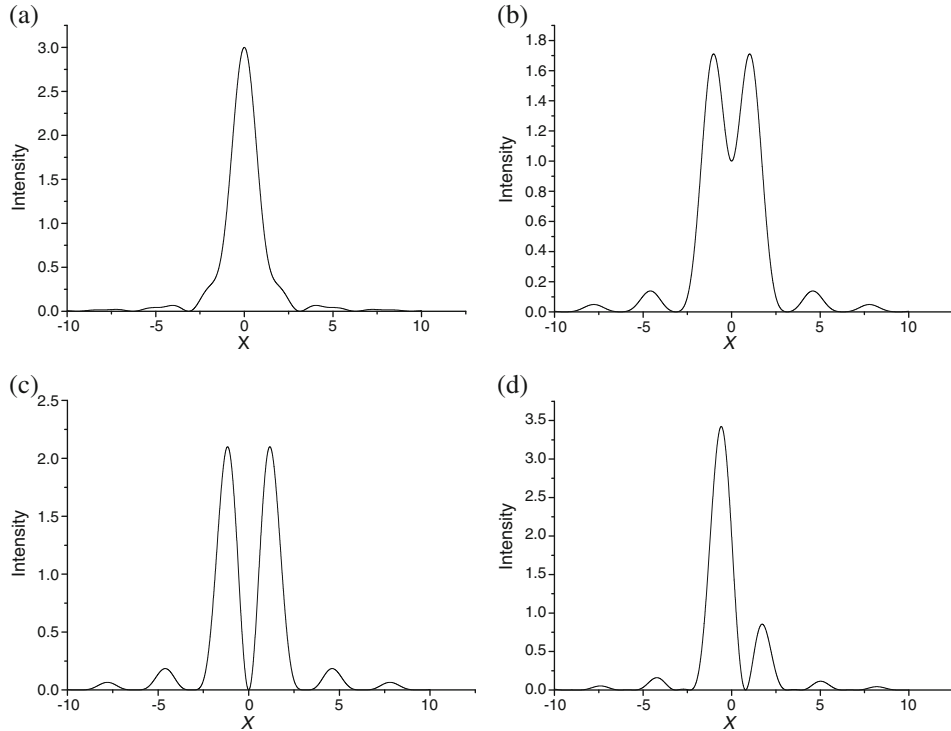


Figure 5. Variation of intensity with X when (a) $a = 1, b = 1, \delta_0 = 0^\circ, \delta = 180^\circ, \Delta_0 = 0, \theta = 30^\circ$, (b) when $a = 1, b = 1, \delta_0 = 0^\circ, \delta = 180^\circ, \Delta_0 = 0, \theta = 60^\circ$, (c) when $a = 1, b = 1, \delta_0 = 0^\circ, \delta = 180^\circ, \Delta_0 = 0, \theta = 90^\circ$ (d) $a = 1, b = 1, \delta_0 = 90^\circ, \delta = 180^\circ, \Delta_0 = 0, \theta = 90^\circ$.

this case the maximum peak is obtained at the centre of the diffraction pattern. Figures 4b–4f depict the variation of intensity distribution for different parameters.

From eq. (15) when $2r = d$, the corresponding intensity distributions are shown in figures 5a–5d for different states of polarization, analyser angles θ and the retardance. The intensity profile is equivalent to that produced by the single aperture of width $2d$. If we assume $2r = 0$, the intensity profile is the same as obtained from the single aperture of width d which has already been depicted in figure 4a.

3. Conclusion

It has been shown that the diffraction pattern of single slit in Case 1 and double slit in Case 2 masked by a polarizing device in both cases can be modified using the polarization properties of light. The study reveals the potentiality of suitably modifying the characteristics of an optical system using vector properties of light. This suggests that polarization Fourier optics offers higher degrees of freedom in manipulating the diffraction behaviour of an aperture and implies that the polarization Fourier optics will be much

more versatile than scalar Fourier optics. Besides, the polarization Fourier optics bears the promise of useful applications in image processing as well.

References

- [1] A K Chakraborty and H Mukherjee, *J. Opt. (India)* **5**, 71 (1976)
- [2] A Ghosh, J Basu, P P Goswami and A K Chakraborty, *J. Mod. Opt.* **34**, 281 (1987)
- [3] A Ghosh, K Murata and A K Chakraborty, *J. Opt. Soc. Am.* **A5**, 277 (1988)
- [4] K Bhattacharya, A Ghosh and A K Chakraborty, *J. Mod. Opt.* **40**, 379 (1993)
- [5] K Bhattacharya, A Ghosh and A K Chakraborty, *J. Opt.* **20**, 128 (1991)
- [6] D Roy Chowdhury, K Bhattacharya, A K Chakraborty and R Ghosh, *Appl. Opt.* **43**, 750 (2004)
- [7] S Sanyal, P Bandyopadhyay and A Ghosh, *Opt. Engng.* **37(2)**, 592 (1998)
- [8] S R Dashiell and A W Lowmann, *Opt. Commun.* **8**, 100 (1973)
- [9] A Ghosh and A K Chakraborty, *Optica Acta* **30**, 425 (1983)
- [10] M Tahir, K Bhattacharya, A Ghosh and A K Chakraborty, *Opt. Rev.* **16(5)**, 1 (2009)
- [11] I Moreno, Marria J Yzuel, J Campos and A Vargas, *J. Mod. Opt.* **51(14)**, 2031 (2004)